International Journal of Electronic and Electrical Engineering.
ISSN 0974-2174, Volume 7, Number 6 (2014), pp. 609-616

http://www.irphouse.com

Performance analysis for DFIG Feeding a Stand-alone Unbalanced Load

Sagar U. Shinde[1] and K. Vadirajacharya[2]

[1,2]Department of Electrical Engineering,
Dr. Babasaheb Ambedkar Technological University, Lonere

Abstract

In this paper, a control system for the operation of a doubly fed induction generator (DFIG), feeding an unbalanced three-phase load is presented. The load unbalance is compensated using the front-end converter. The control system is based on positive and negative sequence components of current. MATLAB Simulation results obtained from a DFIG system and are presented and discussed in this paper.

Keywords> DFIG, predictive current control, GSC-RSC, unbalanced load.

1. Introduction

The Doubly fed induction machine (DFIM), is an induction machine with both stator and rotor windings. A large amount of recently installed windmills is variable-speed turbines, and they use electronics converters in order to operate at different speed rates. The DFIG is one of the main techniques used in variable speed windmills. In this paper the DFIG is used to supply electrical energy to unbalanced stand-alone loads and also the voltage at the output of the combination is determined which can be fed it to the grid system. In this case, negative sequence currents are generated, producing electrical torque pulsations and localized heating in the machine.

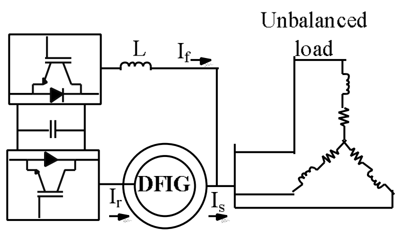

Fig. 1: DFIG sourcing a stand-alone unbalanced load.

This paper proposes the control system for compensating the effect of the unbalanced load. Compensation is achieved by regulating the negative sequence current supplied from the front end converter. This drives the negative sequence currents in the DFIG to zero, thereby, eliminating the torque pulsations.

2. Description of the DFIG

A DFIG can supply power at constant voltage and constant frequency while its rotor rotation speed varies [3–7]. This represents an asset in providing more flexibility in power conversion and also better stability in frequency and voltage control in the power systems to which such generators are connected. A DFIG consists of a wound rotor induction generator (WRIG) with the stator windings directly connected to the three-phase grid/load and the rotor windings connected to a back-to-back partially rated [8–17] power converter. The size of the converter relates not only to the total generator power but also to the selected speed range or the slip power. PWM converters have been widely used. In this paper the cascaded H-bridge multilevel inverter is used for back to back conversion.

Use of the positive and negative reference frame rotating at the speed ω_s and - ω_s is the most common method to analyze the DFIG model. The stationary frames $\alpha_s\beta_s$ and the $\alpha_r\beta_r$ are the rotating frames rotating at the speed ω_r. The PCC method is based on the analysis of rotor voltages v_{rdq} and stator φ_{sdq}, rotor fluxes φ_{rdq}.

$$\varphi_{rd}^{+} = L_r i_{rd}^{+} + L_m i_{sd}^{+} = \frac{L_m^{2}}{L_s} i_{ms} + \sigma L_r i_{rd}^{+} \quad (1)$$

$$\varphi_{rq}^{+} = L_r i_{rq}^{+} + L_m i_{sq}^{+} = \sigma L_r i_{rq}^{+} \quad (2)$$

$$\upsilon_{rd}^{+} = R_r i_{rd}^{+} + \sigma L_r \frac{d}{dt} i_{rd}^{+} - \omega_{sl}^{+} \sigma L_r i_{rq}^{+} \quad (3)$$

$$\upsilon_{rq}^{+} = R_r i_{rq}^{+} + \sigma L_r \frac{d}{dt} i_{rq}^{+} + \omega_{sl}^{+} \left(\frac{L_m^{2}}{L_s} i_{ms} + L_r i_{rd}^{+}\right) \quad (4)$$

Where, R_r, L_m, L_r, L_s, , i_{ms} are the nominal values of rotor resistance, mutual inductance, rotor inductance, stator inductance, total leakage factor, and stator magnetizing current of the generator, respectively.

3. Proposed PCC for unbalanced stand-alone DFIG system

PCC forces the rotor output current follow the reference rotor current. The DFIG stator and the load are star-connected with the neutral points connected, to provide a path for the circulation of zero-sequence currents. The initial excitation for the system start up could be provided by a battery bank (not shown in the figure). The battery could be kept charged afterward using the energy flow in the dc link. Another possibility is to use a bank capacitor in the stator for the self-excitation of the machine, generating the required stator voltage. Then, the control strategy of the line side converter or, in this case, the stator-side converter, could regulate the required dc-link voltage. To compensate the load unbalance, the GSC and/or the RSC can be used. The positive &

negative-sequence vector control system is oriented along the stator voltage vector. The reference rotor current is generated by an outer voltage control loop and a negative sequence component, added to compensate for stator voltage unbalances.

The rotor current in the k[th] sampling period can be estimated based on the current values and the system model.

$$\Delta i^+{}_{rd}(k) = -\frac{T_s R_r}{\sigma L_r} i^+{}_{rd}(k) + \frac{T_s V^+{}_{rd}}{\sigma L_r} + T_s \omega_{sl}(k) i^+{}_{rd}(k) \quad (5)$$

$$\Delta i^+{}_{rq}(k) = -\frac{T_s R_r}{\sigma L_r} i^+{}_{rq}(k) + \frac{T_s V^+{}_{rq}}{\sigma L_r} - T_s \omega_{sl}(k) \left(i^+{}_{rd}(k) + \frac{L^2{}_m}{\sigma L_r L_s} i_{ms}(k) \right) \quad (6)$$

$$\bar{V}^+{}_{rd}(k) = R_r i^+{}_{rd}(k) + \frac{\sigma L_r}{T_s} \Delta i^+{}_{rd}(k) - \omega_{sl} \sigma L_r i^+{}_{rq}(k) \quad (7)$$

$$\bar{V}^+{}_{rq}(k) = R_r i^+{}_{rq}(k) + \frac{\sigma L_r}{T_s} \Delta i^+{}_{rq}(k) + \omega_{sl} \left(\frac{L^2{}_m}{L_s} i_{ms}(k) + \sigma L_r i^+{}_{rd}(k) \right) \quad (8)$$

In order to regulate the output rotor current to follow its reference at the end of the next switching period, the average required output rotor voltages $\bar{v}^+{}_{rdq}(k)$ should be precisely predicted in the next switching period; and they are shown in the discrete basis as (7) and (8). These predicted rotor voltages are then applied into the RSC to force the rotor current error to zero. The compensation method for such time delay should be adopted to avoid large overshoot and oscillations in the rotor current. To increase the control performance in terms of low distortion and low current ripple, the required rotor voltage is then controlled using SVPWM technique.

4. Implementation of SVPWM for Converters

By comparing the stationary frame d-q components of the reference voltage vector, the sector where the reference voltage vector is located is identified. Using the d-q components of the reference voltage vector, a sine loop voltage and a dc-link voltage information, the effective times T_1, T_2 are calculated. Instead of the sine table, to reduce the calculation time, another look-up table which contains the corresponding to each sector number may be used. Using the corresponding sector information the actual switching time for each inverter leg is generated from the combination of effective times and zero sequence time.

$$(|V_{sr}| cos\alpha) * T_s = V_{dc} * T_1 + (V_{dc} cos 60^0) * T_s \quad (9)$$

Equating volt-seconds along the β axis:

$$(|V_{sr}| sin\alpha) * T_s = (V_{dc} sin 60^0) * T_2 \quad (10)$$

Solving the above two simultaneous equations, one gets:

$$T_1 = \frac{|V_{sr}| T_s \sin\left(\frac{\pi}{3} - \alpha\right)}{V_{dc} \sin\left(\frac{\pi}{3}\right)} \quad T_2 = \frac{|V_{sr}| T_s \sin(\alpha)}{V_{dc} \sin\left(\frac{\pi}{3}\right)} \quad (11)$$

$|V_{sr}|$ represents the length of the reference Vector and □ is measured from the start of the vector.

$$T_1 = \frac{2T_s\left[V_\alpha \sin\left(\frac{\pi}{3}\right) - V_\beta \cos\left(\frac{\pi}{3}\right)\right]}{\sqrt{3}V_{dc}} \quad T_2 = \frac{2T_s V_\beta}{\sqrt{3}V_{dc}} \tag{12}$$

Substituting,

$$V_\alpha = \frac{3}{2}V_a^* \quad V_\beta = \frac{\sqrt{3}}{2}(V_b^* - V_c^*) \tag{13}$$

$$T_1 = \frac{T_s(V_a^* - V_b^*)}{V_{dc}} \quad T_2 = \frac{T_s(V_b^* - V_c^*)}{V_{dc}} \tag{14}$$

The imaginary switching periods T_{as}, T_{bs} and T_{cs} are defined as:

$$T_{as} = \left(\frac{T_s}{V_{dc}}\right)V_a^*;\ T_{bs} = \left(\frac{T_s}{V_{dc}}\right)V_b^*;\ T_{cs} = \left(\frac{T_s}{V_{dc}}\right)V_c^* \tag{15}$$

The active vector switching times T_1 and T_2 in sector1 may be expressed as:

$$T_1 = T_{as} - T_{bs};\ T_1 = T_{bs} - T_{cs} \tag{16}$$

Extending this procedure, for the other sectors, the active vector switching times (T_1 and T_2) and for the respective sectors may be expressed in terms of the imaginary switching times (T_{as}, T_{bs} and T_{cs}) for a particular sampling interval. The effective time T_{eff} is the time during which the active vectors are switched in a sector and is given by (T_1 + T_2). This may be determined as the difference between the maximum and minimum values among T_{as}, T_{bs} and T_{cs}. Hence, $T_0 = T_s - T_{eff}$.

$$T_{eff} = \max\{T_{as}, T_{bs}, T_{cs}\} - min\{T_{as}, T_{bs}, T_{cs}\} = T_{max} - T_{min}$$

The offset time, T_{offset} required to distribute the zero voltage symmetrically during one sampling period is given by:

$$T_{offset} = \frac{T_0}{2} - T_{min} \tag{17}$$

The actual switching times for each the inverter leg can be obtained by the time shifting operation as follows:

$$T_{ga} = T_{as} + T_{offset};\ T_{gb} = T_{bs} + T_{offset};\ T_{gc} = T_{cs} + T_{offset} \tag{18}$$

5. Simulation Results

The MATLAB Simulation has been performed for the following system parameters:

DFIG Parameters: 1.5 MW, 575V, 6 pole, 50 Hz.

Battery Parameters: 375V.

Back to back converters: 3 level svpwm cascaded H-bridge converter.

Unbalanced load: 330 ohm, 30 milliHenry

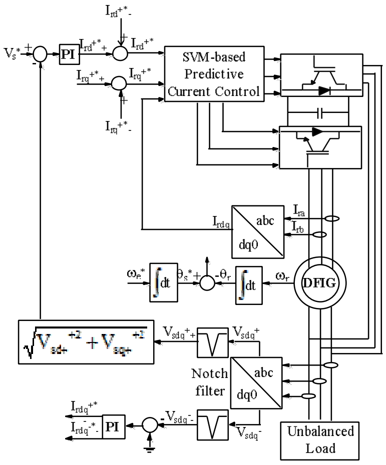

Fig. 2: Simulation diagram

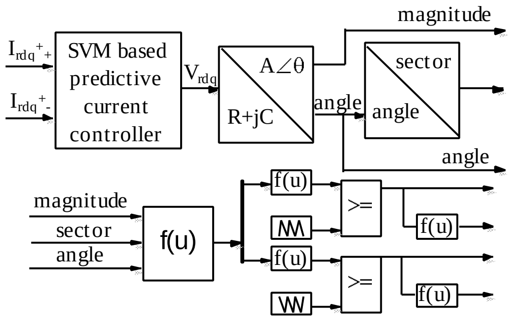

Fig. 3. SVPWM-based Predictive current control circuit

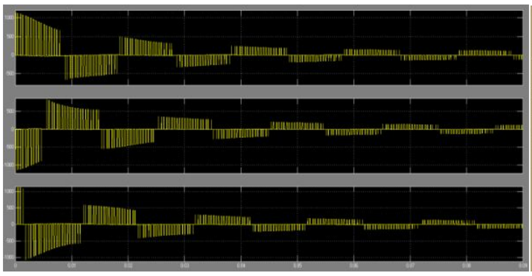

Fig. 4: Rotor side voltage

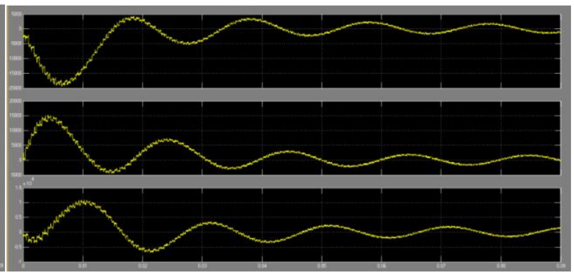

Fig. 5: Rotor side current

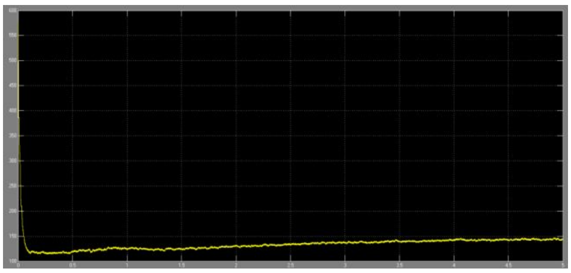

Fig. 5: DC link voltage

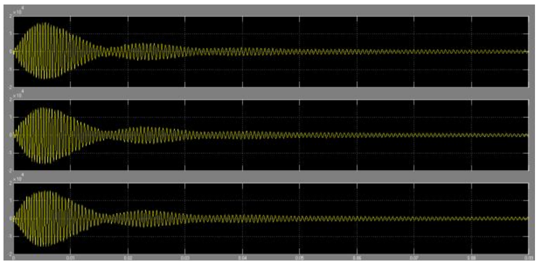

Fig. 6: Voltages at the common point of Rotor side and Stator side.

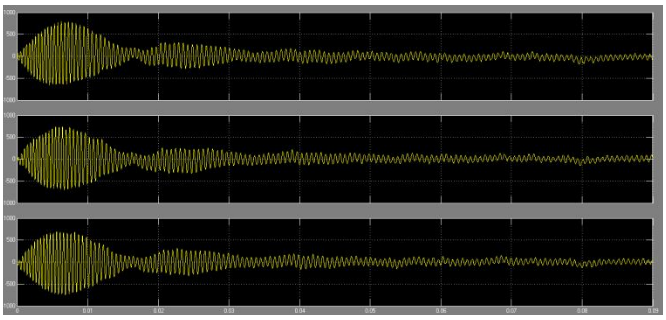

Fig. 7: Currents at the common point of Rotor side and Stator side.

6. Conclusion

An improved PCC method for an unbalanced stand-alone DFIG system has been proposed in this paper and the combined voltages from stator and rotor side converter is calculated as nearly 1200-1500V & 100-130A, for 325 volt battery/caparitor bank which is the addition of the stator side and rotor side voltages, giving the effectiveness and robustness of the proposed control scheme.

References

[1] W. Leonhard, *Control of Electrical Drives*. New York, NY, USA: Springer-Verlag, 2001.
[2] B. Bose, *Modern Power Electronics and AC Drives*. Englewood Cliffs, NJ, USA: Prentice-Hall, 2002.
[3] PENA R., CLARE J.C., ASHER G.M.: ‘A doubly fed inductiongenerator using back-to-back PWM converters supplyingan isolated load from a variable speed wind turbine’, IEE Proc. Electr. Power Appl., 1996, 143, (5), pp. 380–387
[4] BOLDEA I.: ‘Variable speed generators: the electricalhandbook’ (Taylor and Francis, New York, USA, 2006)
[5] LIAO Y., PUTRUS G.A., SMITH K.S.: ‘Evaluation of the effects of rotor harmonics in a doubly-fed induction generator with harmonic induced speed ripple’, IEEE Trans. Energy Convers., 2003, 18, (4), pp. 508–515
[6] CADIRCI I., ERMIS M.: ‘Commutation angle analysis of a double output induction generator operating in sub- and super synchronous modes’. Proc. Seventh IEEE Mediterranean Electrotechnical Conf., 1994, vol. 2, pp. 793–796
[7] SEMAN S., NIIRANEN J., KANERVA S., ARKKIO A.: ‘Analysis of a 1.7MVA doubly fed wind-power induction generator during power system disturbances’. Proc. Nordic Workshop on Power and Industrial Electronics, June 2004
[8] BOLDEA I.: ‘Control of electric generators: a review’. IEEE 26th Annual Industrial Electronics Society Conf., 2003, vol. 1, pp. 972–980
[9] HOFFMAN W., OKAFOR F.: ‘Optimal power utilization with doubly fed full controlled induction generator’. Proc. Sixth IEEE Africon Conf., October 2002, vol. 2, pp. 693–698
[10] RAMOS C.J., MARTINS A.P., ARAUJO A.S., CARVALHO A.S.: ‘Current control in the grid connection of the double-output induction generator linked to a variable speed wind turbine’. IEEE 28th Annual Conf., 2002, vol. 2, pp. 979–984
[11] PETERSON A., LUNDBERG S., THIRINGER T.: ‘A DFIG wind turbine ride through system influence on the energy production’. Nordic Wind Power Conf., March 2004, pp. 1–7
[12] ZHI D., XU L.: ‘Direct power control of DFIG with constant switching frequency and improved transient performance’, IEEE Trans. Energy Convers., 2007, 22,(1), pp. 110–118

[13] XU L., CARTWRIGHT P.: 'Direct active and reactive power control of DFIG for wind energy generation', IEEE Trans. Energy Convers., 2006, 21, (3), pp. 750–758

[14] BOZHKO S.V., GIMNEZ R.B., LI R., CLARE J.C., ASHER G.M.: 'Control of offshore DFIG-based wind farm grid with line commutated HVDC connection', IEEE Trans. Energy Convers., 2007, 22, (1), pp. 71–78

[15] PENA R., CRDENAS R., ESCOBAR E., CLARE J., WHEELER P.: 'Control system for unbalanced operation of stand-alone doubly fed induction generators', IEEE Trans. Energy Convers., 2007, 22, (2), pp. 544–545

[16] Pena, R.; Cardenas, R.; Escobar, E.; Clare, J.; Wheeler, P, "Control System for Unbalanced Operation of Stand-Alone Doubly Fed Induction Generators," IEEE Trans. Energy Conversion, vol.22, no.2, pp.544-545, June 2007.

[17] Pena, R.; Cardenas, R.; Escobar, E.; Clare, J.; Wheeler, P, "Control strategy for a doubly fed induction generator feeding an unbalanced grid or stand-alone load," Electric Power Systems Research, vol. 79, no. 2, pp. 355-264, July 2009.